SCIENTIFIC REPORTS

OPEN

Investigating the Effects of the Interaction Intensity in a Weak Measurement

Received: 13 December 2017
Accepted: 13 April 2018
Published online: 03 May 2018

Fabrizio Piacentini[1], Alessio Avella[1], Marco Gramegna[1], Rudi Lussana[2], Federica Villa[2], Alberto Tosi[2], Giorgio Brida[1], Ivo Pietro Degiovanni[1] & Marco Genovese[1]

Measurements are crucial in quantum mechanics, for fundamental research as well as for applicative fields like quantum metrology, quantum-enhanced measurements and other quantum technologies. In the recent years, weak-interaction-based protocols like Weak Measurements and Protective Measurements have been experimentally realized, showing peculiar features leading to surprising advantages in several different applications. In this work we analyze the validity range for such measurement protocols, that is, how the interaction strength affects the weak value extraction, by measuring different polarization weak values on heralded single photons. We show that, even in the weak interaction regime, the coupling intensity limits the range of weak values achievable, setting a threshold on the signal amplification effect exploited in many weak measurement based experiments.

The fundamental role of measurement in quantum mechanics is undisputed[1], since it is the process in which some of the distinctive traits of the quantum world with respect to the classical one appear: e.g., the fact that quantum states collapse in a specific eigenstate of the observable (corresponding to the measured eigenvalue) when a strong measurement (described by a projection operator) is performed, causing the impossibility to measure non-commuting observables on the same particle.

However, in recent years a new paradigm of quantum measurement emerged, in which the coupling strength between the measured quantum state and the measurement system is weak enough to prevent the wave function collapse (at the cost of extracting only a small amount of information from a single measurement). It is the case of Weak Measurements (WMs), introduced in[2,3] and firstly realized in[4–6], and Protective Measurements (PMs), originally proposed within the debate on the reality of the wave function[7] and recently realized for the first time[8].

WMs can give rise to anomalous (imaginary and/or unbounded) values, whose real part is regarded as a conditional average of the observable in the zero-disturbance limit[9], while the imaginary one is related to the disturbance of the measuring pointer during the measurement[10]. Beyond having inspired a significant analysis of the meaning of quantum measurement[11–18], they have been used both to address foundational problems[19], like macrorealism[20–22] and contextuality[23–25], and as a novel, impressive tool for quantum metrology and related quantum technologies allowing high-precision measurements (at least in presence of specific noises[26,27]), as the tiny spin Hall effect[6] or small beam deflections[28–31] and characterization of quantum states[32,33]. Furthermore, the absence of wave function collapse in WMs allows performing sequential measurements of even non-commuting observables on the same particle[34–37], a task forbidden within the strong measurement framework in quantum mechanics.

On the other hand, PMs combine the weak interaction typical of WMs with some protection mechanism preserving the initial state from decoherence. Although a very controversial and debated topic from the foundational perspective[38–48], PMs have demonstrated unprecedented measurement capability, allowing to extract the quantum expectation value of an observable in a single measurement on a single (protected) particle[8], a task usually forbidden in quantum mechanics.

Both of these protocols require a von Neumann interaction with a very weak coupling between the observable to be measured and the pointer observable, rising the issue of when the regime of weak interaction approximation can be considered valid[49,50]. For instance, this is of the utmost relevance specially when dealing with anomalous weak values, for which the weakness of the von Neumann interaction is crucial for the reliability of the measurement, giving rise to a signal amplification effect already demonstrated in several experiments[6,26–31].

[1]Istituto Nazionale di Ricerca Metrologica, Strada delle Cacce 91, 10135, Torino, Italy. [2]Politecnico di Milano, Dipartimento di Elettronica, Informazione e Bioingegneria, Piazza Leonardo da Vinci 32, 20133, Milano, Italy. Correspondence and requests for materials should be addressed to M. Genovese (email: m.genovese@inrim.it)

Up to now, a generic theoretical discussion of this point has been carried out in[51–59], while a few papers[60–65] have afforded an experimental investigation of this issue for specific physical systems. In this work we aim at investigating the specific case of polarization weak measurements, both for its widespread application[66–70] and as an emblematic example of general considerations. For this purpose, we have realized a single-photon-based experiment studying the response of the weak value measurement process in different conditions and observing, for a given interaction strength, the limits in which the expected weak value can be accurately extracted. Up to our knowledge, this is the first time for such an experiment to be run at the single particle level, the regime which WMs really belong to.

We show how the von Neumann coupling intensity intrinsically provides some boundaries on the range of weak values that one is able to determine without abandoning the weak interaction approximation, setting, as a consequence, a threshold on the signal amplification effect mentioned above.

Theoretical framework

The weak value of an observable $\hat{A}$ is defined as $\langle\hat{A}\rangle_w = \frac{\langle\psi_f \mid \hat{A} \mid \psi_i\rangle}{\langle\psi_f \mid \psi_i\rangle}$, where $|\psi_i\rangle$ and $|\psi_f\rangle$ are the pre- and post-selected quantum states, respectively[2]. To extract the weak value, one usually implements a von Neumann indirect measurement coupling the observable of interest (OoI) $\hat{A}$ to a pointer observable $\hat{P}$ by means of the unitary operation $\hat{U} = e^{-ig\hat{A}\otimes\hat{P}}$, being g the von Neumann coupling strength. After a post-selection onto the state $|\psi_f\rangle$, realized by the projector $\hat{\Pi}_f = |\psi_f\rangle\langle\psi_f|$, the information on the OoI is obtained by measuring the meter observable $\hat{Q}$, canonically conjugated with the pointer $\hat{P}$.

Let us focus on the case of a single qubit, and take as OoI a projection operator of the form $\hat{A} = |\psi_A\rangle\langle\psi_A|$. Considering the initial state $|\psi_i\rangle = |\psi_i\rangle \otimes |\phi(q)\rangle$, after the von Neumann interaction and the subsequent post-selection the final state is:

$$|\Psi_f\rangle = \hat{\Pi}_f\hat{U}|\Psi_i\rangle = z\left[\mathbb{I} + \langle\hat{A}\rangle_w\left(e^{-ig\hat{P}} - \mathbb{I}\right)\right]|\psi_i\rangle \otimes |\phi(q)\rangle \tag{1}$$

being $z = \langle\psi_f|\psi_i\rangle$ the internal product between the pre- and post-selected state.

Then, considering as initial condition $\langle\phi(q)|\hat{Q}|\phi(q)\rangle = 0$, the expectation value of the meter observable $\hat{Q}$ onto the final state can be written as:

$$\begin{aligned}\langle\Psi_f|\hat{Q}|\Psi_f\rangle \;=\; & |z|^2\left\{2Re\left[\langle\hat{A}\rangle_w\langle\phi(q)|\hat{Q}e^{-ig\hat{P}}|\phi(q)\rangle\right]\right. \\ & \left. + |\langle\hat{A}\rangle_w|^2\left(g - 2Re\left[\langle\phi(q)|\hat{Q}e^{-ig\hat{P}}|\phi(q)\rangle\right]\right)\right\}.\end{aligned} \tag{2}$$

In the limit of weak interaction ($g \to 0$), the first perturbative order of the right term in Eq. (2) is:

$$|z|^2 g\{Re[\langle\hat{A}\rangle_w] + Im[\langle\hat{A}\rangle_w]\langle\phi(q)|(\hat{Q}\hat{P} + \hat{P}\hat{Q})|\phi(q)\rangle\}. \tag{3}$$

Hence, restricting ourselves to the case of real weak values, Eq. (2) gives:

$$\langle\Psi_f|\hat{Q}|\Psi_f\rangle = |z|^2 g\langle\hat{A}\rangle_w \tag{4}$$

showing how the (real) weak value of our OoI A can be obtained by a measurement of the meter Q, canonically conjugated with the pointer P. Going further in the series expansion, one finds that the contribution at the second order is null, so the next non-trivial contribution scales as g^3.

In our experiment we extract the weak value of the polarization of single photons, collimated in a Gaussian mode $|\phi(q)\rangle = \int dq f(q)|q\rangle$, with $f(q) = (2\pi\sigma^2)^{-\frac{1}{4}}\exp\left(-\frac{q^2}{4\sigma^2}\right)$. The $Im[\langle\hat{A}\rangle_w] = 0$ constraint is satisfied by restricting to pre- and post-selected states of the form $|\psi_j\rangle = \cos\theta_j|H\rangle + \sin\theta_j|V\rangle$, where H (V) indicates the horizontal (vertical) polarization and $j = i, f$ the pre- and post-selected state. As pointer observable we choose the transverse momentum $\hat{P}_Q$ in the direction Q (orthogonal to the photon propagation direction), $\hat{Q}$ being our meter observable.

Experimental implementation

The single photons exploited in our experiment are produced by a heralded single-photon source[71,72] in which a 76 MHz Ti:Sapphire mode-locked laser at 796 nm is frequency doubled via second harmonic generation and then injected into a 5 mm thick $LiIO_3$ nonlinear crystal, generating photon pairs via type-I Parametric Down-Conversion (PDC), as reported in Fig. 1.

The idler photon ($\lambda_i = 920$ nm) is filtered by an interference filter (IF), coupled to a single mode fiber (SMF) and detected by a silicon single-photon avalanche diode (Si-SPAD). A click from the Si-SPAD heralds the presence of the signal photon ($\lambda_s = 702$ nm) in the correlated branch. Such photon passes through an IF, then is SMF coupled and addressed, collimated in a Gaussian mode, to the open air path where the WMs take place. We have verified our single photon emission by measuring the antibunching parameter[73] of our source, obtaining a value of 0.13(1) without any background/dark-count subtraction.

In such path, the heralded single photon is prepared in the linearly-polarized state $|\psi_i\rangle = \frac{1}{\sqrt{2}}(|H\rangle + |V\rangle)$ by means of a polarizing beam splitter (PBS) followed by a half wave plate. After the state preparation, the photon encounters a pair of thin birefringent crystals, responsible for the weak interactions. The first birefringent crystal (BC_V) presents an extraordinary (e) optical axis lying in the Y-Z plane, with an angle of $\pi/4$ with respect to the Z direction. The spatial walk-off induced on the photons by BC_V slightly shifts the vertically-polarized ones,

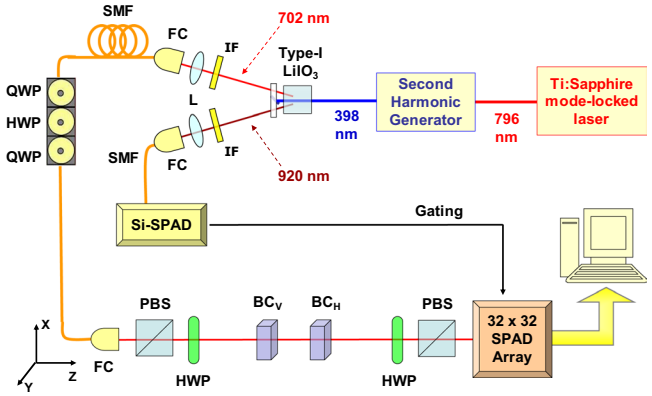

Figure 1. Experimental setup. Heralded single photons are produced by downconversion in a 5-mm long type-I $LiIO_3$ non-linear crystal; the pump beam, obtained by second harmonic generation of a mode-locked laser (rep. rate 76 MHz), produces idler ($\lambda_i = 920$ nm) and signal ($\lambda_s = 702$ nm) photons, which pass through interference filters (IFs) before being coupled to single-mode fibres (SMFs). The idler photons are detected by means of a Silicon single-photon avalanche diode (Si-SPAD), sending a trigger pulse to the signal photons detection system, Signal photons are prepared in the initial polarization state $|\psi_i\rangle$ by means of a polarising beam splitter (PBS) and a half-wave plate (HWP), then they pass through a birefringent crystal BC_V shifting them in the transverse Y direction, depending on their polarisation, thus measuring $\hat{\Pi}_V$ weakly. Subsequently, an identical birefringent crystal (BC_H), performs the weak measurement of $\hat{\Pi}_H$ by shifting the photons along the X direction. The final post-selection onto the state $|\psi_f\rangle$ is determined by a HWP followed by a PBS. At the end of the optical path, the heralded photons are detected by a spatial-resolving 32×32 SPAD array.

separating horizontal- and vertical-polarization paths along the Y direction and causing the initial state $|\psi_i\rangle$ to be affected by a small amount of decoherence. This element realizes the first (weak) interaction $\hat{U}_V = e^{-ia_y \hat{\Pi}_V \otimes \hat{P}_y}$, coupling the observable under test (i.e. the vertical polarization $\hat{\Pi}_V = |V\rangle\langle V|$) to the pointer observable, the transverse momentum along the Y direction $\hat{P}_y$.

Then, the photon goes through the second birefringent crystal (BC_H), identical to the first one, but with the e-axis lying in the X-Z plane. Here, the photons experiencing the spatial walk-off are the horizontally-polarized ones. They are shifted along the X direction and the initial polarization state undergoes the same decoherence induced by the passage in BC_V. This way, the second (weak) interaction $\hat{U}_H = e^{-ia_x \hat{\Pi}_H \otimes \hat{P}_x}$ occurs. This configuration allows measuring simultaneously the weak values of the two orthogonal polarizations $\hat{\Pi}_V$ and $\hat{\Pi}_H$, at the same time self-compensating the unwanted temporal walk-off induced by the two interactions.

After the two birefringent crystals, the photon undergoes the postselection, that is, a projection onto the final state $|\psi_f\rangle$ realized by a half wave plate followed by a PBS.

The final photon detection is performed by a spatial resolving single-photon detector prototype, i.e. a two-dimensional array made of 32×32 "smart pixels" (each hosting a SPAD detector with dedicated front-end electronics for counting and timing single photons) operating in parallel with a global shutter readout[74]. Each count by the Si-SPAD on the heralding arm triggers a 6 ns detection window in each pixel of the SPAD array, in order to heavily decrease the dark count rate and improve the signal-to-noise ratio.

We perform two different acquisitions, respectively with 1 mm and 2.5 mm thick birefringent crystals, in order to change the coupling strength of the weak interactions experienced by the single photons. In each acquisition, we variate the postselection state and measure different weak values, observing the behaviour of the meter variables with respect to the weak values theoretically predicted.

Results and Conclusions

For each pair of birefringent crystals, we perform an initial system calibration to determine the von Neumann coupling intensity g, obtaining for the 1-mm long crystals $a_x = a_y = 0.7$ pixels (px), while $a_x = 1.9$ px and $a_y = 1.7$ px for the 2.5-mm long ones (the small discrepancy between a_x and a_y is due to a slight mismatch in the birefringent crystals cut). Considering that our single photons are collimated in a Gaussian distribution whose width parameter is $\sigma = 4.3$ px, the two birefringent crystal pairs induce respectively an interaction strength of $g_x = g_y = a_y/\sigma \simeq 0.16$ and $g_y = a_y/\sigma \simeq 0.40$ and $g_x = a_x/\sigma \simeq 0.45$. These conditions should still lie within the weak interaction regime, since for all of them $g^2 \ll 1$.

The results obtained with the 1-mm and 2.5-mm birefringent crystal pairs are reported in Figs 2 and 3, respectively. In each of these figures, plots (a) and (b) report the behavior of the meter observables $\langle \hat{X} \rangle$ and $\langle \hat{Y} \rangle$ with respect to the theoretical weak values associated to them ($\langle \hat{\Pi}_H \rangle_w$ and $\langle \hat{\Pi}_V \rangle_w$, respectively). The orange (purple) dots are the measured values of $\langle \hat{X} \rangle$ ($\langle \hat{Y} \rangle$), the solid curve represents the exact solution of Eq. (2) while the dotted line and the dashed curve indicate respectively the first order approximation, corresponding to the weak value $\langle \hat{\Pi}_H \rangle_w$ ($\langle \hat{\Pi}_V \rangle_w$), and the third order one in the $g^2 \ll 1$ limit (we remind the reader that the second order approximation gives null contribution).

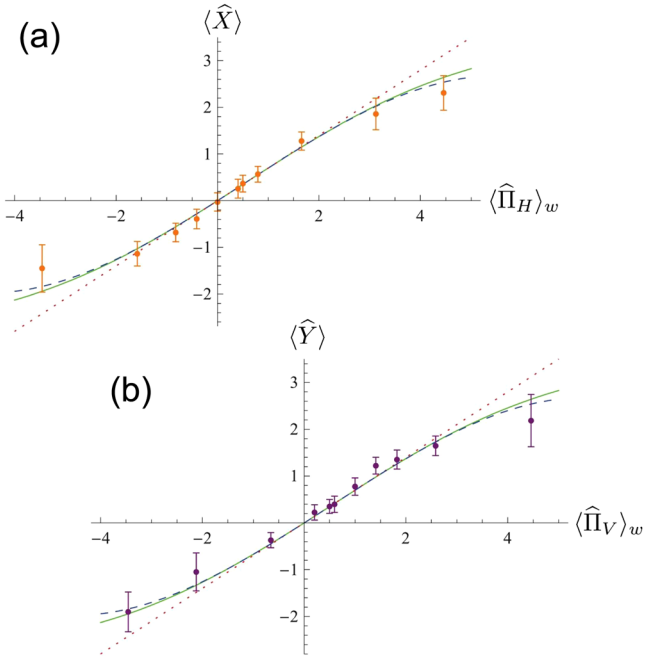

Figure 2. Obtained results for the acquisition with the 1-mm long birefringent crystal pair. Plot (**a**) (**b**): behavior of the meter observable $\hat{X}$ ($\hat{Y}$) with respect to the expected weak value $\langle \hat{\Pi}_H \rangle_w$ ($\langle \hat{\Pi}_V \rangle_w$). Dots: experimental data. Solid green curve: complete theory of the von Neumann coupling occurring in the birefringent crystal. Dashed curve: third order approximation of the complete theory in the limit of weak coupling ($g^2 \ll 1$). Dotted line: first order approximation of the complete theory for $g^2 \ll 1$, the one used for the weak value evaluation.

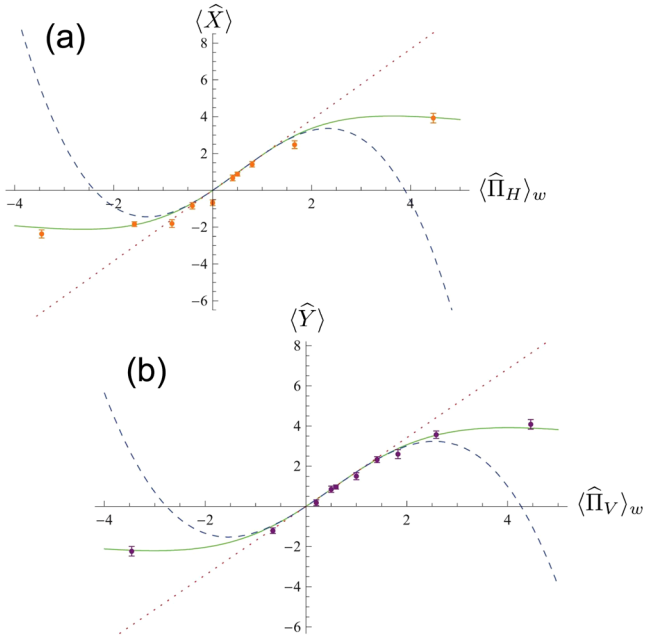

Figure 3. Obtained results for the acquisition with the 2.5-mm long birefringent crystal pair. Plot (**a**) (**b**): behavior of the meter observable $\hat{X}$ ($\hat{Y}$) with respect to the expected weak value $\langle \hat{\Pi}_H \rangle_w$ ($\langle \hat{\Pi}_V \rangle_w$). Dots: experimental data. Solid green curve: complete theory of the von Neumann coupling occurring in the birefringent crystal. Dashed curve: third order approximation of the complete theory in the limit of weak coupling ($g^2 \ll 1$). Dotted line: first order approximation of the complete theory for $g^2 \ll 1$, the one used for the weak value extraction.

As visible in Fig. 2, obtained in the condition $g \simeq 0.16$ with the 1 mm birefringent crystals, the weak value approximation is valid for a good range of anomalous values, that is, for $\langle \hat{\Pi}_H \rangle_w$, $\langle \hat{\Pi}_V \rangle_w \in [-1.5, 2.5]$ (region I). Outside this interval, the data start following the third order approximation and the exact solution, almost indistinguishable in the investigated range (region II). This means that, outside region I, a bias begins to affect our weak value estimation.

The situation becomes different when we switch to the 2.5-mm long BC_H and BC_V, increasing the interaction strength almost to the border of the weak interaction regime. By looking at Fig. 3, we can identify three regions: region I, corresponding to $\langle \hat{\Pi}_H \rangle_w$, $\langle \hat{\Pi}_V \rangle_w \in [-0.7, 1.7]$, for which the meter observables still follow the weak value approximation; region II, for $\langle \hat{\Pi}_H \rangle_w$, $\langle \hat{\Pi}_V \rangle_w \in [-1.2, -0.7] \vee [1.7, 2.2]$, in which the third order approximation (dashed line) is still valid; region III (absent in Fig. 2), corresponding to $\langle \hat{\Pi}_H \rangle_w$, $\langle \hat{\Pi}_V \rangle_w < -1.2 \vee \langle \hat{\Pi}_H \rangle_w$, $\langle \hat{\Pi}_V \rangle_w > 2.2$, in which the exact solution assumes a quasi-asymptotic form and both approximations fail. In this last region, our meter observables $\langle \hat{X} \rangle$ and $\langle \hat{Y} \rangle$ remain basically constant with respect to $\langle \hat{\Pi}_H \rangle_w$ and $\langle \hat{\Pi}_V \rangle_w$, hence it is not possible anymore to extract the weak value.

In summary, while in region I in principle one can safely estimate the weak value, in region II the bias due to the finite interaction intensity already affects such estimation, completely forbidding it in region III. This means that the signal amplification effect exploited in many WM-based experiments[6,26–31] is actually limited to a certain range of weak values, determined by the parameter to be evaluated, i.e. the interaction intensity g, and indeed these results were used for choosing the settings of refs[22,24,36]. Outside of such interval, the weak value approximation can no longer be considered valid, forbidding any accurate weak value measurement and, as a consequence, leading to an unfaithful g extraction due to biased signal amplification.

In the end, we experimentally investigated the limits of WMs, observing how, even in the weak interaction regime, the value of g determines the range of weak values that one is able to extract, putting a threshold to the signal amplification effect[6,26–31] typical of WMs. From our data it results evident that even a very weak coupling, satisfying the constraint $g^2 \ll 1$, could lead to a bias in the weak value measurement in the case of strongly anomalous values. This means that, to determine an unknown weak coupling intensity exploiting the signal amplification mentioned before, we have to be sure not to cross the borders of the first order solution of Eq. (2). Supposing of not having any "a priori" information on g, the only robust strategy to do so is to perform a wide range of measurements for different weak values until the same picture reported in Figs 2 and 3 appears, and then pick only the values belonging to the weak approximation region.

Giving a deeper insight on weak value measurements and their properties, our results pave the way to their widespread diffusion in several applicative fields, e.g. quantum metrology, quantum-enhanced measurement and related quantum technologies.

References

1. Genovese, M. Interpretations of Quantum Mechanics and Measurement Problem. *Adv. Sci. Lett.* **3**, 244 (2010).
2. Aharonov, Y., Albert, D. Z. & Vaidman, L. How the result of a measurement of a component of the spin of a spin-1/2 particle can turn out to be 100. *Phys. Rev. Lett.* **60**, 1351–1354 (1988).
3. Tamir, B. & Cohen, E. Introduction to Weak Measurements and Weak Values. *Quanta* **2**, 7–17 (2013).
4. Ritchie, N. W. M., Story, J. G. & Hulet, R. G. Realization of a measurement of a "weak value". *Phys. Rev. Lett.* **66**, 1107–1110 (1991).
5. Pryde, G. J., O'Brien, J. L., White, A. G., Ralph, T. C. & Wiseman, H. M. Measurement of quantum weak values of photon polarization. *Phys. Rev. Lett.* **94**, 220405 (2005).
6. Hosten, O. & Kwiat, P. Observation of the Spin Hall Effect of Light via Weak Measurements. *Science* **319**, 787–790 (2008).
7. Aharonov, Y. & Vaidman, L. Measurement of the Schrödinger Wave of a Single Particle. *Phys. Lett. A* **178**, 38 (1993).
8. Piacentini, F. *et al*. Determining the quantum expectation value by measuring a single photon. *Nat. Phys.* **13**, 1191–1194 (2017).
9. Dressel, J., Agarwal, S. & Jordan, A. N. Contextual Values of Observables in Quantum Measurements. *Phys. Rev. Lett.* **104**, 240401 (2010).
10. Dressel, J. & Jordan, A. N. Significance of the imaginary part of the weak value. *Phys. Rev. A* **85**, 012107 (2012).
11. Vaidman, L. Weak value controversy. *Phil. Trans. A*, https://doi.org/10.1098/rsta.2016.0395 (2017).
12. Hall, M. J. W., Pati, A. K. & Wu, J. Products of weak values: Uncertainty relations, complementarity, and incompatibility. *Phys. Rev. A* **93**, 052118 (2016).
13. Diosi, L. Structural features of sequential weak measurements. *Phys. Rev. A* **94**, 010103 (2016).
14. Vaidman, L. *et al*. Weak value beyond conditional expectation value of the pointer readings. *Phys. Rev. A* **96**, 032114 (2017).
15. Wang, Y., Hou, J., Qi, X. Quantum correlation based on weak measurements. *Int. J. of Quant. Inf.* https://doi.org/10.1142/S0219749917500411 (2017).
16. Aharonov, Y., Cohen, E. & Elitzur, A. C. Foundations and applications of weak quantum measurements. *Phys. Rev. A* **89**, 052105 (2014).
17. Aharonov, Y., Cohen, E. & Elitzur, A. C. Can a future choice affect a past measurements outcome? *Ann. of Phys.* **355**, 258–268 (2015).
18. Oreshkov, O. & Brun, T. A. Weak Measurements Are Universal. *Phys. Rev. Lett.* **95**, 110409 (2005).
19. Aharonov, Y., Botero, A., Popescu, S., Reznik, B. & Tollaksen, J. Revisiting Hardy's paradox: counterfactual statements, real measurements, entanglement and weak values. *Phys. Lett. A* **301**, 130–138 (2002).
20. Williams, N. S. & Jordan, A. N. Weak Values and the Leggett-Garg Inequality in Solid-State Qubits. *Phys. Rev. Lett.* **100**, 026804 (2008).
21. Goggin, M. E. *et al*. Violation of the Leggett-Garg inequality with weak measurements of photons. *Proc. Natl. Acad. Sci. USA* **108**, 1256–1261 (2011).
22. Avella, A. *et al*. Anomalous Weak Values and the Violation of a Multiple-measurement Leggett-Garg Inequality. *Phys. Rev. A* **96**, 052123 (2017).
23. Pusey, M. Anomalous Weak Values Are Proofs of Contextuality. *Phys. Rev. Lett.* **113**, 200401 (2014).
24. Piacentini, F. *et al*. Experiment Investigating the Connection between Weak Values and Contextuality. *Phys. Rev. Lett.* **116**, 180401 (2016).
25. Waegell, M. *et al*. Confined Contextuality in Neutron Interferometry: Observing the Quantum Pigeonhole Effect. *Phys. Rev. A* **96**, 052131 (2017).
26. Dressel, J., Malik, M., Miatto, F. M., Jordan, A. N. & Boyd, R. W. Colloquium: Understanding quantum weak values: Basics and applications. *Rev. Mod. Phys.* **86**, 307–316 (2014).
27. Hallaji, M., Feizpour, A., Dmochowski, G., Sinclair, J. & Steinberg, A. M. Weak-value amplification of the nonlinear effect of a single photon. *Nat. Phys.* **13**, 540–544 (2017).
28. Resch, K. J. Amplifying a Tiny Optical Effect. *Science* **319**, 733–734 (2008).

29. Dixon, P. B., Starling, D. J., Jordan, A. N. & Howell, J. C. Ultrasensitive Beam Deflection Measurement via Interferometric Weak Value Amplification. *Phys. Rev. Lett.* **102**, 173601 (2009).
30. Hogan, J. M. *et al*. Precision angle sensor using an optical lever inside a Sagnac interferometer. *Opt. Lett.* **36**, 1698 (2011).
31. Magana-Loaiza, O. S., Mirhosseini, M., Rodenburg, B. & Boyd, R. W. Amplification of Angular Rotations Using Weak Measurements. *Phys. Rev. Lett.* **112**, 200401 (2014).
32. Salvail, J. Z. *et al*. Full characterization of polarization states of light via direct measurement. *Nat. Phot.* **7**, 316 (2013).
33. Lundeen, J. S., Sutherland, B., Patel, A., Stewart, C. & Bamber, C. Direct measurement of the quantum wavefunction. *Nature* **474**, 188 (2011).
34. Mitchison, G., Jozsa, R. & Popescu, S. Sequential weak measurement. *Phys. Rev. A* **76**, 062105 (2007).
35. Thekkadath, G. S. *et al*. Direct measurement of the density matrix of a quantum system. *Phys. Rev. Lett.* **117**, 120401 (2016).
36. Piacentini, F. *et al*. Measuring Incompatible Observables by Exploiting Sequential Weak Values. *Phys. Rev. Lett.* **117**, 170402 (2016).
37. Putz, G., Barnea, T. J., Gisin, N. & Martin, A. Experimental weak measurement of two non-commuting observables. arXiv:1610.04464 (2016).
38. Rovelli, C. Comment on "Meaning of the wave function". *Phys. Rev. A* **50**, 2788–2792 (1994).
39. Unruh, W. G. Reality and measurement of the wave function. *Phys. Rev. A* **50**, 882–887 (1994).
40. D'Ariano, G. M. & Yuen, H. P. Impossibility of measuring the wave function of a single quantum system. *Phys. Rev. Lett*. **76**, 2832–2835 (1996).
41. Aharonov, Y., Anandan, J. & Vaidman, L. The Meaning of Protective Measurements. *Found. Phys.* **26**, 117–126 (1996).
42. Dass, N. H. & Qureshi, T. Critique of protective measurements. *Phys. Rev. A* **59**, 2590–2601 (1999).
43. Uffink, J. How to protect the interpretation of the wave function against protective measurements. *Phys. Rev. A* **60**, 3474–3481 (1999).
44. Gao, S. Protective Measurement and Quantum Reality (Cambridge University Press, UK, 2015).
45. Aharonov, Y., Englert, B. G. & Scully, M. O. Protective measurements and Bohm trajectories. *Phys. Lett. A* **263**, 137–146 (1999).
46. Diosi, L. Determination of the stationary basis from protective measurement on a single system. In [44], pp. 63–67 (2015).
47. Schlosshauer, M. Measuring the quantum state of a single system with minimum state disturbance. *Phys. Rev. A* **93**, 012115 (2016).
48. Aharonov, Y. & Vaidman, L. Protective Measurements of Two-State Vectors. In *Potentiality, Entanglement and Passion-at-a-Distance*, eds/ R. S. Cohen, M. Horne and J. Stachel, BSPS1–8, quant-ph/9602009 (Kluwer, 1997).
49. Shikano, Y. & Hosoya, A. Weak values with decoherence. *Journal of Physics A* **43**, 025304 (2010).
50. Kofman, A. G., Ashhab, S. & Nori, F. Nonperturbative theory of weak pre- and post-selected measurements. *Physics Reports* **520**, 43–133 (2012).
51. Wiseman, H. M. Weak values, quantum trajectories, and the cavity-QED experiment on wave-particle correlation. *Phys. Rev. A* **65**, 032111 (2002).
52. Geszti, T. Postselected weak measurement beyond the weak value. *Phys. Rev. A* **81**, 044102 (2010).
53. Parks, A. D. & Gray, J. E. Variance control in weak-value measurement pointers. *Phys. Rev. A* **84**, 012116 (2011).
54. Di Lorenzo, A. Full counting statistics of weak-value measurement. *Phys. Rev. A* **85**, 032106 (2012).
55. Susa, Y., Shikano, Y. & Hosoya, A. Optimal probe wave function of weak-value amplification. *Phys. Rev. A* **85**, 052110 (2012).
56. Wu, S. & Zukowski, M. Feasible Optical Weak Measurements of Complementary Observables via a Single Hamiltonian. *Phys. Rev. Lett.* **108**, 080403 (2012).
57. Dressel, J., Lyons, K., Jordan, A. N., Graham, T. M. & Kwiat, P. G. Strengthening weak-value amplification with recycled photons. *Phys. Rev. A* **88**, 023821 (2013).
58. Dressel, J. & Jordan, A. N. Weak Values are Universal in Von Neumann Measurements. *Phys. Rev. Lett.* **109**, 230402 (2012).
59. Kumari, A., Kumar Pan, A. & Panigrahi, P. K. Joint weak value for all order coupling using continuous variable and qubit probe. *Eur. Phys. J. D* **71**, 275 (2017).
60. Martínez-Rincón, J., Mullarkey, C. A., Viza, G. I., Liu, W.-T. & Howell, J. C. Ultrasensitive inverse weak-value tilt meter. *Optics Letters* **42**, 2479–2482 (2017).
61. Starling, D. J., Ben Dixon, P., Williams, N. S., Jordan, A. N. & Howell, J. C. Continuous phase amplification with a Sagnac interferometer. *Phys. Rev. A* **82**, 011802(R) (2010).
62. Xu, X.-Y. *et al*. Phase Estimation with Weak Measurement Using a White Light Source. *Phys. Rev. Lett.* **111**, 033604 (2013).
63. Martínez-Rincón, J., Liu, W.-T., Viza, G. I. & Howell, J. C. Can Anomalous Amplification be Attained without Postselection? *Phys. Rev. Lett.* **116**, 100803 (2016).
64. Martínez-Rincón, J., Chen, Z. & Howell, J. C. Practical advantages of almost-balanced-weak-value metrological techniques. *Phys. Rev. A* **95**, 063804 (2017).
65. Liu, W.-T., Martínez-Rincón, J., Viza, G. I. & Howell, J. C. Anomalous Amplification of a Homodyne signal via Almost-Balanced Weak Values. *Opt. Lett.* **42**, 903–906 (2017).
66. Cho, Y.-W., Lim, H.-T., Ra, Y.-S. & Kim, Y.-H. Weak value measurement with an incoherent measuring device. *New Journal of Physics* **12**, 023036 (2010).
67. Zhou, X., Ling, X., Zhang, Z., Luo, H. & Wen, S. Observation of Spin Hall Effect in Photon Tunneling via Weak Measurements. *Scientific Reports* **4**, 7388 (2014).
68. Zhou, X., Xiao, Z., Luo, H. & Wen, S. Experimental observation of the spin Hall effect of light on a nanometal film via weak measurements. *Phys. Rev. A* **85**, 043809 (2012).
69. Jayaswal, G., Mistura, G. & Merano, M. Observing angular deviations in light beam reflection via weak measurements. *Opt. Lett.* **39**, 6257 (2014).
70. Fang, C., Huang, J.-Z., Yu, Y., Li, Q. & Zeng, G. Ultra-small time-delay estimation via a weak measurement technique with post-selection. *J. Phys. B: At. Mol. Opt. Phys.* **49**, 175501 (2016).
71. Castelletto, S., Degiovanni, I. P., Schettini, V. & Migdall, A. Spatial and spectral mode selection of heralded single photons from pulsed parametric down-conversion. *Opt. Expr.* **13**(18), 6709 (2005).
72. Brida, G. *et al*. Improved implementation of the AlickiVan Ryn nonclassicality test for a single particle using Si detectors. *Phys. Rev. A* **79**, 044102 (2009).
73. Grangier, P., Roger, G. & Aspect, A. Experimental Evidence for a Photon Anticorrelation Effect on a Beam Splitter: A New Light on Single-Photon Interferences. *Eur. Phys. Lett.* **1**, 173 (1986).
74. Villa, F. *et al*. CMOS Imager With 1024 SPADs and TDCs for Single-Photon Timing and 3-D Time-of-Flight. *IEEE J. Sel. Top. Quantum Electron.* **20**, 3804810 (2014).

Acknowledgements

This work has been supported by EMPIR-14IND05 "MIQC2" and EMPIR-17FUN01 "Become" (the EMPIR initiative is co-funded by the EU H2020 and the EMPIR Participating States) and the MIUR Progetto Premiale 2014 "Q-SecGroundSpace". We thank Dr. Mattia P. Levi for contributing to the experimental setup implementation and data analysis.

Author Contributions

I.P.D., M. Gram and M. Gen (responsible of the laboratories) planned the experiment. The experimental realization was achieved (supervised by I.P.D., G.B., M. Gram and M. Gen) by F.P. (leading role) and A.A. The camera was developed and optimized for this experiment by R.L., F.V., A.T. The manuscript was prepared with inputs by all the authors. They also had a fruitful systematic discussion on the progress of the work.

Additional Information

Competing Interests: The authors declare no competing interests.

Publisher's note: Springer Nature remains neutral with regard to jurisdictional claims in published maps and institutional affiliations.